Fundamentals of airborne gamma-ray spectrometry

Article *in* AGSO journal of Australian geology & geophysics · January 1997

CITATIONS
129

READS
254

1 author:

Brian Minty
Minty Geophysics
47 PUBLICATIONS **759** CITATIONS

SEE PROFILE

AGSO Journal of Australian Geology & Geophysics, 17(2), 39–50

Fundamentals of airborne gamma-ray spectrometry

B.R.S. Minty[1]

The interpretation of gamma-ray spectrometric data requires an understanding of the underlying physics of the method, and an insight into the data acquisition, system calibration, and data processing and presentation procedures. The shape and intensity of a measured airborne gamma-ray spectrum is a complex function of many variables. Source thickness, source diameter, the detector response, and the distance between the source and the detector all affect the measured spectrum. The approach taken to calibration, therefore, is empirical. The source and detector are viewed as a single system, and the response of this system to changes in aircraft height (to obtain attenuation coefficients) and sources of known geometry and concentration (to obtain sensitivity coefficients) is measured. These empirically determined constants are, however, only valid for the source and source–detector geometry used in the calibration process.

Introduction

Airborne gamma-ray spectrometry requires consideration of many variables. For example, in addition to the geometry and physical property contrasts of the radioactive sources, the measured gamma radiation is a function of the size, efficiency and speed of the detector. It is also dependent on environmental and other effects, such as soil moisture, rainfall, vegetation, non-radioactive overburden, and the movement of airborne sources of radiation in the lower atmosphere. Interpretation of gamma-ray spectrometric data requires an understanding of the underlying physics of the method, and an insight into the data acquisition, system calibration, and data processing and presentation procedures. Effective interpretation also needs consideration of disequilibrium conditions in the uranium decay series, and an insight into the chemistry of potassium (K), uranium (U), and thorium (Th) in the natural environment.

The purpose of this paper is to review the fundamentals of airborne gamma-ray spectrometry. Basic radioactivity and the sources of gamma radiation are reviewed. This is followed by discussion on the interaction of gamma rays with matter, the response of an airborne detector system, and the properties of measured airborne gamma-ray spectra—including factors that affect the shape of measured spectra. The use of mathematical models of the gamma-ray field for survey design, data processing and interpretation are then briefly reviewed. The paper concludes with a discussion of the application of the method, including the corrections that must be applied to field data.

The review is intended to provide an insight into the theoretical and practical aspects of airborne gamma-ray spectrometry needed for an understanding of calibration and data-processing procedures.

Basic radioactivity

Some isotopes are unstable and change to more stable nuclei by the emission of energetic ionising radiation. These isotopes are called radioactive isotopes or radioisotopes. Each radioisotope has a characteristic probability associated with the radioactive disintegration of its nuclei. This is the so-called 'half-life' of the isotope and is the time taken for half the nuclei to decay. Thus after one half-life, half the original radioactive isotopes remain, and after two half-lives, one quarter of the original radioactive isotopes remain, and so on.

The three main types of radiation arising from radioactive decay are alpha, beta, and gamma rays. Alpha rays (or alpha particles) are fragments of the original nuclei and consist of 2 protons and 2 neutrons. They have a discrete energy, and the emitting isotope can be identified by this energy. Since alpha particles have both a charge and mass, they are easily absorbed by a few centimetres of air. Beta particles are identical to electrons and carry a unit negative charge. They do not have a characteristic energy. Beta particles are less easily absorbed than alpha particles and can travel up to a metre in air.

The emission of an alpha or beta particle usually leaves the new nucleus in an excited state and the surplus energy is radiated as gamma rays. These are quanta or photons of energy which are very penetrating because they possess neither charge nor mass. Gamma rays can penetrate up to 30 cm of rock and several hundred metres of air, and are the only choice available for the remote sensing of terrestrial radioactivity. Each gamma-ray photon has a discrete energy, and this energy is characteristic of the source isotope. This forms the basis of gamma-ray spectrometry, i.e. the measurement of gamma-ray photon energy allows the source of the radiation to be diagnosed. Energies of geological interest lie between 0.2 and 3 MeV, which corresponds to electromagnetic wavelengths of about 3×10^{-12} m and a frequency of about 3×10^{19} Hz.

The radioactivity decay law

While it is impossible to predict the exact moment at which a particular atom will decay, each radioisotope has a characteristic rate of disintegration, which is proportional to the number of nuclei present. Thus the number of nuclei (dN) which decay during a short time (dt) is proportional to the number of nuclei present (N). i.e.

$$\frac{dN}{dt} = -\lambda N \tag{1}$$

or

$$N = N_0 e^{-\lambda t} \tag{2}$$

where λ is the decay constant, N_0 is the number of radionuclides present at time $t = 0$, and N is the number of nuclides present after a time t. A related constant is the previously mentioned 'half-life'. When $N = \frac{1}{2} N_0$ we have

$$t_{\frac{1}{2}} = \frac{0.693}{\lambda} \tag{3}$$

Usually, the activity of the source (number of disintegrations per unit time) is measured, and the activity also decreases exponentially over time with the same half-life as that used in equation 2.

Multiple decay and chain disintegration

Some radionuclides have more than one mode of decay. For example, 64 per cent of ^{212}Bi disintegrations are by alpha particle emission to ^{212}Po, and 34 per cent are by beta particle emission to ^{208}Th. But irrespective of the type of radiation we are measuring, the observed half-life is always the same.

Radioactive decay often occurs in a series (or chain) with a number of daughter products, which are also radioactive, and terminates in a stable isotope. In this case, the net rate at which a daughter changes is the difference between the rate at which it is produced and the rate at which it decays. The growth of a radioactive daughter from its radioactive parent is thus controlled by the half-lives of both isotopes.

[1] Australian Geological Survey Organisation, GPO Box 378, Canberra, ACT 2601

Sources of gamma-radiation

The sources of natural gamma-radiation can be conveniently divided into 3 groups, according to their origin (Kogan et al. 1969). The first group includes ^{40}K, ^{238}U, ^{235}U and ^{232}Th, which are believed to have been synthesised during the creation of the universe and have half-lives of the same order as the age of the earth (5×10^9 years). The second group comprises radioactive isotopes that are daughter products from the decay of isotopes in the first group. These have half-lives ranging from small fractions of a second to 10^4–10^5 years. The third group would include isotopes created by external causes, such as the interaction of cosmic rays with the Earth and its atmosphere.

Natural sources of radiation

Potassium, U, and Th are the only naturally occurring elements with radioisotopes that produce gamma rays of sufficient energy and intensity to be measured at airborne survey heights. Average crustal abundances are K—2%, U—2.7ppm, Th—8.5ppm. These elements have been decaying continually since their creation, and their concentration in the Earth is, therefore, continually decreasing. But these isotopes have very long half-lives and, therefore, are still relatively abundant. The decay of these radioisotopes and their daughters is sometimes accompanied by gamma-ray emissions.

^{40}K is the only radioactive isotope of K, and occurs as 0.012 per cent of natural K. Eighty-nine per cent of ^{40}K nuclei decay by electron emission (i.e. beta particle) to ^{40}Ca, while the remaining 11 per cent decay by electron capture to ^{40}Ar. This is followed by the emission of a single gamma-ray photon with energy 1.46 MeV. Since ^{40}K occurs as a fixed proportion of K in the natural environment, the gamma-ray flux from ^{40}K can, therefore, be used to estimate the total amount of K present. K is a much weaker source of radiation than the U or Th series, but because it is so abundant (2%), it is found to be an equal contributor to U and Th in the natural radiation flux.

Uranium occurs naturally as the radioisotopes ^{238}U and ^{235}U, which give rise to decay series that terminate in the stable isotopes ^{206}Pb and ^{207}Pb, respectively (Tables 1, 2). ^{238}U has a half-life of 4.47×10^9 years. The half-life of ^{235}U is 7.13×10^8 years. Since these half-lives are not the same, it follows that the ratio $^{235}U/^{238}U$ is changing very slowly with time. ^{235}U forms only 0.72 per cent of naturally occurring U and the gamma-ray energies in its decay series are too low to be diagnostic in airborne gamma-ray surveying.

Thorium occurs naturally as the radioisotope ^{232}Th, which gives rise to a decay series that terminates in the stable isotope ^{208}Pb (Table 3).

Note that neither ^{238}U nor ^{232}Th emit gamma rays, and we thus rely on the gamma-ray emissions from their radioactive daughter products to estimate their concentrations.

Disequilibrium

Disequilibrium in the U decay series is a serious source of error in gamma-ray spectrometric surveying. When radioactive decay results in an unstable daughter product with a half-life shorter than that of the parent, a situation will eventually be reached where the daughter product is decaying as rapidly as it is being produced. If this is true for all the daughters in a decay series, then the series is said to be in secular equilibrium, and the total activity decreases at the same rate as that of the original parent. Note that equal activity under equilibrium conditions does not imply equal concentration, since the relevant half-lives must be considered when calculating the relative concentration of members of a decay series.

Disequilibrium occurs when one or more decay products are completely or partially removed or added to the system, and it may take days, weeks or even millions of years to restore equilibrium, depending on the half-lives of the radioisotopes involved. Thorium rarely occurs out of equilibrium in nature, and there are no disequilibrium problems with K, since it only exhibits a single photo-peak. However, in the U decay series, disequilibrium is common in the natural environment. Fractionation can be due to both physical and chemical mechanisms. For example, the nuclear recoil from an atomic disintegration can result in an isotope being moved from its original position in a crystal lattice into a position more accessible to oxidising solutions, such as within microfractures. Examples of chemical mechanisms are coprecipitation (Ra preferentially scavenged from solution by hydroxides of Fe), adsorption (Ra preferentially adsorbed onto the surface of clays), and biological uptake (Ra more readily absorbed into plant tissues than U). Disequilibrium can result from fractionation at (at least) 5 positions in the ^{238}U decay series:

- ^{238}U can be selectively leached relative to ^{234}U, particularly in a clay matrix;
- ^{234}U can be selectively leached relative to ^{238}U;
- ^{230}Th can be selectively leached relative to the other isotopes in the chain;
- ^{226}Ra fractionation; and
- ^{222}Rn (radon gas) is very mobile and can escape into the atmosphere from soil and rock fissures.

Both U and Ra are soluble and, thus, transportable. In an oxidising environment, U is preferentially leached relative to Ra, and in a reducing environment Ra may be preferentially leached relative to U.

If ^{222}Rn escapes, the short-lived nuclides ^{214}Bi and ^{214}Pb, which occur below ^{222}Rn in the U decay series and are the major gamma-ray emitters in this series, will decay to insignificant activities within hours. The time taken for equilibrium to be re-established in this case is about 38 days, as the time needed to restore 99.9 per cent equilibrium for a disturbed member of a series is about 10 times the half-life of the disturbed member. Where there has been preferential leaching of ^{238}U and ^{234}U relative to Ra, it can take up to a million years to re-establish equilibrium. In this case the ^{214}Bi and ^{214}Pb concentrations will remain high for a very long time—even though ^{238}U and ^{234}U may have been completely removed. This is due to the long half-life of ^{230}Th, which intervenes between ^{234}U and $^{214}Bi/^{214}Pb$ in the U decay series (Table 1).

Note that isotopes of Rn also occur in the ^{235}U decay series (^{219}Rn—emanation Actinon) and in the ^{232}Th decay series (^{220}Rn—emanation Thoron). These are not sources of disequilibrium, since their half-lives are very short.

Accurate estimates of U from gamma-ray spectrometry, where we rely on the abundance of isotopes such as ^{214}Bi and ^{214}Pb, which occur far down in the radioactive decay chain, require equilibrium conditions that are frequently not present. These estimates are, therefore, usually reported as 'equivalent uranium' (eU), reminding us that the accuracy of these is dependent on the presence of equilibrium conditions. Thorium is also usually reported as 'equivalent thorium' (eTh), although the Th decay series is almost always in equilibrium.

Background radiation

Any radiation not originating from the ground is regarded as 'background', since it is of no geological significance and needs to be removed from the observed data. There are four sources of background radiation flux—atmospheric radon, cosmic background, aircraft background, and fallout products from atomic explosions and nuclear accidents.

Atmospheric ^{222}Rn and its daughter products, specifically ^{214}Bi and ^{214}Pb, are the major contributors to the background. ^{222}Rn (radon gas) is very mobile and can escape into the atmosphere from soil and rock fissures in response to the 'pumping' action of changing temperature and pressure. Its

Table 1. ^{238}U decay series (simplified after Radiological Health Handbook 1970, and Ivanovich & Harmon 1982).

Nuclide	*Half-life*	*Major radiation energy (MeV) and intensity**					
		α		β		γ	
^{238}U	4.468×10^9 y.	4.15 4.19	(23%) (77%)	–		–	
^{234}Th	24.1 d.	–		~0.103 0.191	(19%) (81%)	0.063 0.093	(3.5%) (4%)
^{234}Pa	1.18 m	–		2.29	(98%)	0.765 1.001	(0.30%) (0.60%)
99.86% / 0.14%							
^{234}Pa	6.7 h	–		0.53 1.13	(66%) (13%)	0.10 0.70 0.90	(50%) (24%) (70%)
^{234}U	2.48×10^5 y.	4.72 4.77	(28%) (72%)	–		0.053	(0.2%)
^{230}Th	7.52×10^4 y.	4.62 4.68	(24%) (76%)	–		0.068 0.142	(0.6%) (0.07%)
^{226}Ra	1602 y.	4.60 4.78	(5.5%) (94.5%)	–		0.186	(4%)
^{222}Rn	3.825 d.	5.49	(~100%)	–		0.510	(0.07%)
^{218}Po	3.05 m	6.11	(100%)	0.33	(100%)	–	
99.98% / 0.02%							
^{214}Pb	26.8 m	–		1.03	(6%)	0.295 0.352	(19%) (36%)
^{218}At	2 s	6.65 6.70	(6%) (94%)	0.67	(94%)	–	
^{214}Bi	19.7 m	5.61	(100%)	3.26	(100%)	0.609 1.120 1.764	(47%) (17%) (17%)
99.96% / 0.04%							
^{214}Po	164 μs	7.83	(100%)	–		0.799	(0.014%)
^{210}Tl	1.32 m	–		2.3	(100%)	0.296 0.795 1.31	(80%) (100%) (21%)
^{210}Pb	~22 y.	3.7	(1.8×10^{-8}%)	0.017 0.064	(85%) (15%)	0.047	(4%)
^{210}Bi	5.02 d.	4.93 4.89 4.59	(60%) (34%) (5%)	1.155	(100%)	–	
~100% / ~.00001%							
^{210}Po	138.3 d.	5.30	(100%)	–		0.803	(0.0011%)
^{206}Tl	4.19 m	–		1.520	(100%)	–	
^{206}Pb	Stable	–		–		–	

* Intensity refers to percentage of disintegrations of the nuclide itself, not to the original parent of the series

daughter products ^{214}Bi and ^{214}Pb attach to airborne aerosols and dust particles and their distribution is thus a function of air movements and wind patterns. Foote (1969) showed that atmospheric background first increased and then decreased during the course of a day, and attributed this to the rise of the near-surface temperature inversion layer and its subsequent break-up in the afternoon. During warm settled weather it is common for atmospheric ^{214}Bi and ^{214}Pb to be at a maximum close to the ground early in the morning and to decrease during the day as increasing air turbulence mixes the lower atmosphere. Temperature inversion layers over topographic depressions and lakes often trap Rn close to the ground and under still air conditions there can be measurable differences in atmospheric radioactivity at sites only a few kilometres apart (Darnley & Grasty 1971).

Primary cosmic radiation from outside our solar system and from the sun reacts with atoms and molecules in the upper atmosphere and generates a complex secondary radiation. This radiation reacts with the air, aircraft and detector to produce the measured 'cosmic' gamma-ray background. In the lower atmosphere, this radiation has a constant energy distribution, but it decreases in amplitude with decreasing altitude (Aviv & Vulcan 1983). The effect of cosmic interaction with rocks is small (Gregory 1960), and variations in cosmic

Table 2. ^{235}U decay series (simplified after Radiological Health Handbook 1970, and Ivanovich & Harmon 1982).

Nuclide	*Half-life*	*Major radiation energy (MeV) and intensity**					
		α		β		γ	
^{235}U	$7.13x10^8$ y.	4.36	(18%)	–		0.143	(11%)
		4.39	(57%)			0.185	(54%)
		4.1-4.6	(8%)			0.204	(5%)
^{231}Th	25.64 h	–		0.300	(~100%)	0.026	(2%)
						0.084	(10%)
^{231}Pa	$3.43x10^4$ y.	5.01	(<20 %)	–		0.027	(6%)
		4.99	(25.4%)			0.29	(6%)
		4.94	(22.8%)				
^{227}Ac	22 y.	4.95	(48.7%)	0.046	(100%)	0.070	(0.08%)
98.8% 1.2%		4.94	(36.1%)				
		4.87	(6.9%)				
^{227}Th	18.17 d.	5.76	(21%)	–		0.050	(8%)
		5.98	(24%)			0.237	(15%)
		6.04	(23%)			0.31	(8%)
^{223}Fr	21 m	5.34	(.005%)	1.15	(100%)	0.050	(40%)
						0.080	(13%)
						0.234	(4%)
^{223}Ra	11.68 d.	5.61	(26%)	–		0.149	(10%)
		5.71	(53.7%)			0.270	(10%)
		5.75	(9.1%)			0.33	(6%)
^{219}Rn	3.92 s	6.42	(8%)	–		0.272	(9%)
		6.55	(11%)			0.401	(5%)
		6.82	(81%)				
^{215}Po	1.83 ms	7.38	(100%)	–		–	
^{211}Pb	36.1 m	–		0.95	(1.4%)	0.405	(3.4%)
				0.53	(5.5%)	0.427	(1.8%)
				1.36	(92.4%)	0.832	(3.4%)
^{211}Bi	2.16 m	6.28	(17%)	0.60	(0.28%)	0.351	(14%)
0.32% 98.68%		6.62	(83%)				
^{211}Po	0.52 s	7.43	(99%)	–		0.570	(0.5%)
						0.90	(0.5%)
^{207}Tl	4.79 m	–		1.44	(100%)	0.897	(0.16%)
^{207}Pb	Stable	–		–		–	

* Intensity refers to percentage of disintegrations of the nuclide itself, not to the original parent of the series

background on a day-to-day basis due to changes in atmospheric pressure are minor (Grasty & Carson 1982).

Aircraft background refers to radiation due to trace amounts of K, U and Th in the aircraft and equipment, as well as the detector itself. This component of background is constant.

The main fallout from nuclear explosions and accidents that affects airborne gamma-ray spectrometry is ^{137}Cs. This exhibits a single photopeak at 0.662 MeV and has a half-life of about 30 years.

Interaction of gamma rays with matter

There are three principal processes by which gamma rays interact with matter—the photoelectric effect, Compton scattering, and pair production.

The ***photoelectric effect*** results in all the energy of the photon being absorbed by the bound electron of an atom (as kinetic energy). This is the predominant absorption process at low energy levels.

Compton scattering is the process whereby an incident

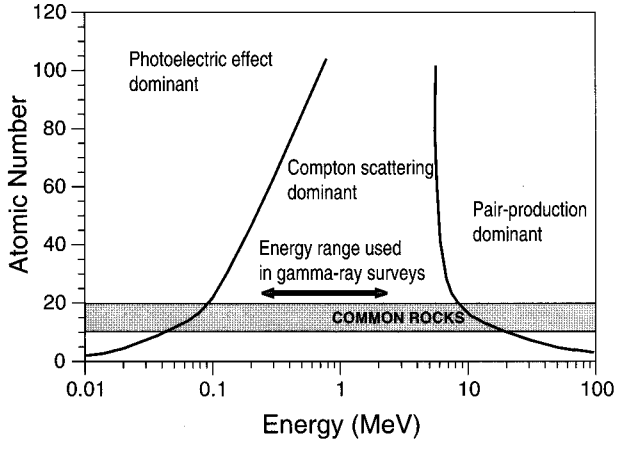

Figure 1. The interaction of gamma rays with matter.

Table 3 ^{232}Th decay series (simplified after Radiological Health Handbook 1970, and Ivanovich & Harmon 1982).

Nuclide	*Half-life*	*Major radiation energy (MeV) and intensity**					
		α		β		γ	
^{232}Th	1.39×10^{10} y.	3.95	(24%)	–		–	
		4.01	(76%)				
↓							
^{228}Ra	5.75 y.	–		0.055	(100%)	–	
^{228}Ac	6.13 h	–		2.11	(100%)	0.34	(15%)
↓						0.908	(25%)
						0.96	(20%)
^{228}Th	1.913 y.	5.34	(28%)	–		0.084	(1.6%)
↓		5.42	(71%)			0.214	(0.3%)
^{224}Ra	3.64 d.	5.45	(5.5%)	–		0.241	(3.7%)
↓		5.68	(94.5%)				
^{220}Rn	55.6 s	6.30	(~100%)	–		0.55	(0.07%)
↓							
^{216}Po	0.145 s	6.78	(100%)	–		–	
↓							
^{212}Pb	10.64 h	–		0.580		0.239	(47%)
↓						0.300	(3.2%)
^{212}Bi	60.5 m	6.05	(70%)	2.25	(100%)	0.040	(2%)
64.0% ↓ 36.0%		6.09	(30%)			0.727	(7%)
						1.620	(1.8%)
^{212}Po	304 ns	8.78	(100%)	–		–	
^{208}Tl	3.1 m	–		1.80	(100%)	0.511	(23%)
						0.583	(86%)
						0.860	(12%)
						2.614	(100%)
↓							
^{208}Pb	Stable	–		–		–	

* Intensity refers to percentage of disintegrations of the nuclide itself, not to the original parent of the series

photon loses part of its energy to an electron, and is 'scattered' at an angle to its original direction. The energy lost by the gamma ray is transferred as kinetic energy to the electron. This is the predominant process for moderate energy levels.

Pair production is the process whereby an incident photon is completely absorbed. This results in the creation of an electron-positron pair in the electrostatic field of a nucleus and with a total energies equal to that of the original photon. This can occur at energy greater than 1.02 MeV and predominates at very high energy and particularly in materials of high atomic number. The life expectancy of the positron is very short. The positron annihilates with an electron producing two 0.511 MeV gamma rays.

Figure 1 illustrates the relationship between these processes, the gamma-ray energy of the incident photon, and the atomic number of the absorbing medium. From this it is clear that Compton scattering is the predominant process for the range of energy and absorbing media encountered in airborne gamma-ray surveying. The gamma-ray photons lose energy through successive Compton scattering events, until eventually the resulting low-energy photons are completely absorbed through the photoelectric effect. Typically, gamma-ray photons in the energy range 0.7–3.0 MeV lose (on average) slightly more than half of their energy during each scattering event. Gamma-ray photons that have been scattered twice will have their energies reduced (on average) to about one-fifth of their original energy (Bailey 1986). Thus, most gamma-ray photons detected in this energy range have either been scattered only once or not at all.

Both Compton scattering and the photoelectric effect are electron collision processes, and the attenuation of gamma rays in most materials encountered in airborne gamma-ray surveying is thus proportional to the electron density of the material. Wood, for example, can be used to shield the detectors from radioactive sources during experiments on the ground, and thus simulate the attenuation of gamma rays by hundreds of metres of air.

Properties of airborne gamma-ray spectra

K and the U and Th equilibrium series each have a characteristic theoretical line spectrum (Figs 2, 3, 4). These line spectra represent the energy distribution of emitted photons at the source. But the energy of these original photons is degraded by Compton scattering in the source, in matter between the source and the detector, and in the detector itself. Figures 5–7 show the simulated gamma-ray flux due to K, U, and Th at 300 m height (Kirkegaard & Lovborg 1974). Each radioelement generates a sharp peak representing the energy of directly transmitted photons. This is superimposed on the spectrum of Compton scattered photons, which show a continuum of energy up to the maximum of the photons emitted by the isotope (e.g. Fig. 5). This continuum is due to single and multiple scattering events between the source and the detector. The gamma-ray flux distributions shown in Figures 6 and 7 are then the sum of the flux spectra for each of the radioelements in the respective decay series. The relative contribution of scattered and unscattered photons to the gamma-ray flux at airborne altitude depends on the source geometry (thickness

and lateral extent) and on the amount of attenuating material between the source and the detector.

The shape of the gamma-ray flux spectrum at airborne heights is thus a function of the concentration of radioelements in the source, the source geometry, the thickness of any non-radioactive overburden, and the height of the detector above the ground. In practice, it is impossible to record the gamma-ray flux spectra shown in Figures 5–7. This is because the shape of the measured spectrum, in addition to the factors mentioned above, is also a function of the detector response. These are discussed below:

The detector response

Tl-doped NaI scintillation crystals are universally used in airborne gamma-ray spectrometry to detect gamma rays. The effect of the scattering and absorption of an incident gamma-ray photon within the detector crystal is the production of one or more highly energetic electrons. NaI(Tl) scintillation crystals have the special property of converting the energy transferred to the electrons into a flash of light. The physical processes

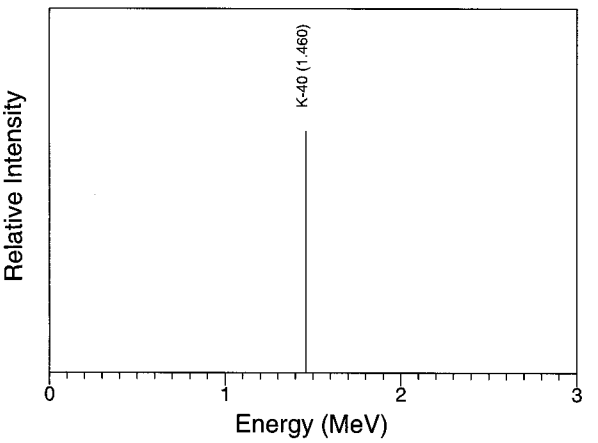

Figure 2. Potassium line spectrum.

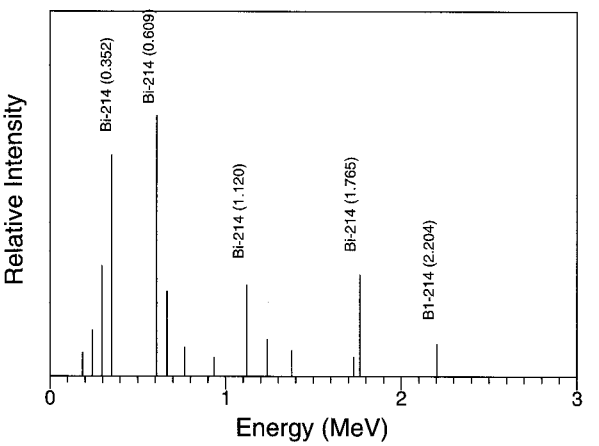

Figure 3. Uranium line spectrum.

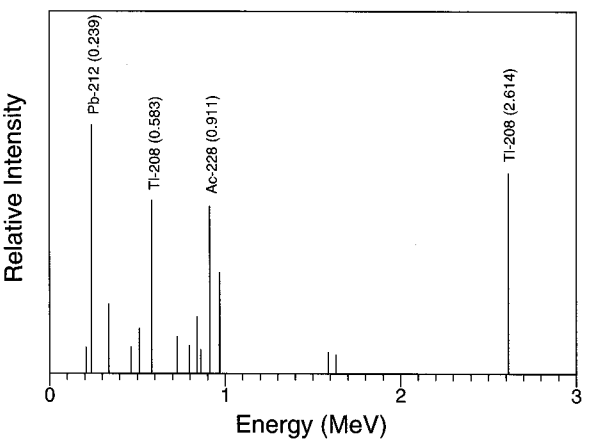

Figure 4. Thorium line spectrum.

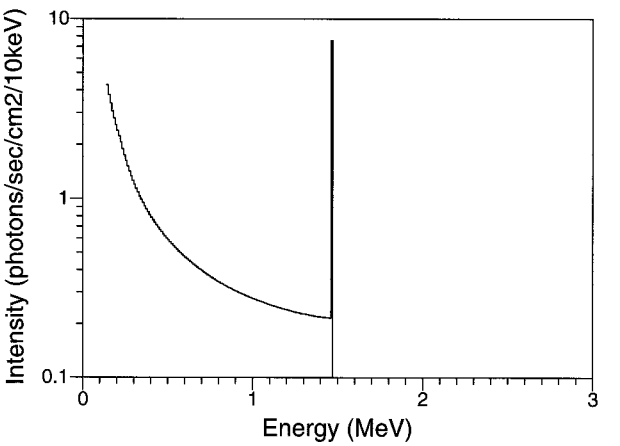

Figure 5. Simulated potassium gamma-ray flux at 300 m altitude.

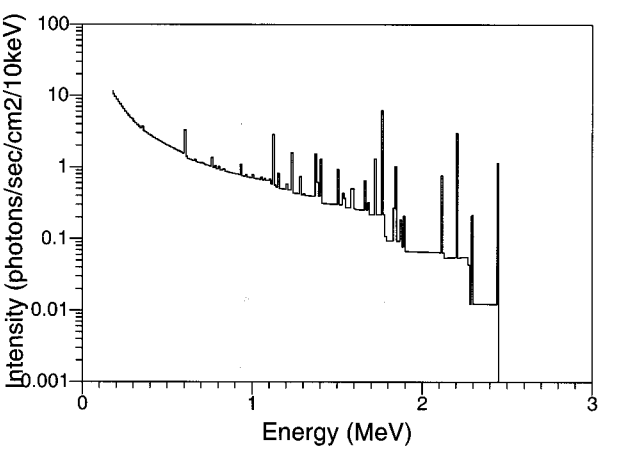

Figure 6. Simulated uranium decay series gamma-ray flux at 300 m

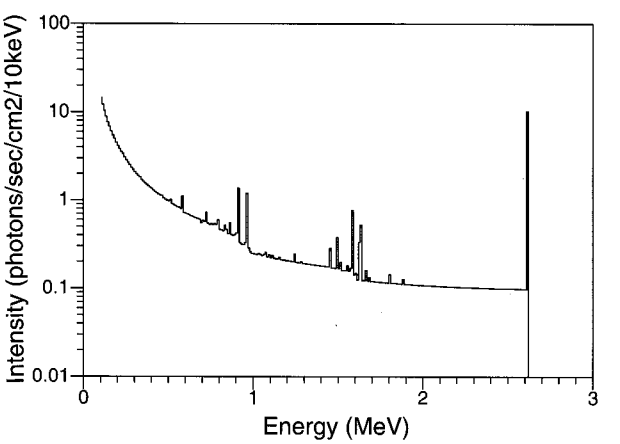

Figure 7. Simulated thorium decay series gamma-ray flux at 300 m altitude.

involved in the scintillation effect are quite complex, and will not be discussed here. Typically, an incident photon might suffer several Compton scattering events within the crystal before being absorbed by the photoelectric effect. The sum of all the photons of visible light released by the process is proportional to the gamma-ray energy of the incident gamma ray.

A photomultiplier tube is attached to the end of each scintillation crystal. Photons of visible light produced in the body of the crystal liberate electrons from the photomultiplier's photocathode. The electrons are multiplied and converted to electrical signals. The amplitude of output pulses from the photomultiplier tubes is proportional to the energy of the original gamma-ray photons.

The airborne gamma-ray detector modifies the spectrum considerably. The main aspects of the detector response are: detector efficiency as a function of energy; directional sensitivity; resolution; dead time; and factors contributing to the shape of the actual pulse height spectrum measured by spectrometers.

Detector efficiency can be considered as a measure of the probability that a photon emitted from the source will interact in the detector with the loss of a finite amount of energy. NaI(Tl) detectors are far more efficient at absorbing low-energy photons than high-energy photons. This is one reason for the higher count rates in the lower-energy channels. Also, slab crystals laid side by side present a greater cross-sectional area to photons approaching from below the aircraft than from the side, and this gives the detector a directional sensitivity.

Detector resolution is a measure of a detector's ability to distinguish between two gamma rays of only slightly different energy. In airborne gamma-ray spectrometry, this is usually defined as the width of a photopeak at half the maximum amplitude divided by the photopeak energy. Typical resolutions are 10% for ^{137}Cs at 0.662 MeV and 7% for ^{208}Tl at 2.615 MeV.

Dead time refers to the finite time required for the spectrometer to process individual photons. This should be as small as possible, since the total counting time available is reduced by the time taken to process all photons detected.

Heath (1964) gave a good summary of ***factors affecting the shape of the pulse amplitude spectrum***, such as escape events, accidental summing, and the characteristic 'Compton edge', representing maximum energy transfer between the photon and a recoil electron. Some photons may escape the detector after being only partially absorbed, and their interaction would result in a measured energy somewhat lower than that of the incident photon ('Compton scatter escape'). In each 'pair-production' event, two 0.51 MeV gamma rays are produced by the annihilation of the positron. Escape of either or both of these photons results in recorded pulses with energy 0.51 MeV and 1.02 MeV less, respectively, than that of the incident photon ('pair-production escape'). This effect can lead to recognisable 'escape peaks' in the spectrum, with energy either 0.51 MeV or 1.02 MeV lower than prominent photopeaks. A similar effect occurs when the 28 keV X-ray given off during the photoelectric process escapes the crystal without further interaction ('x-ray escape'). Also, pair production outside the crystals can result in either or both of the 0.51 MeV photons being detected, to produce 'annihilation radiation peaks'.

Note that the photopeaks in a typical spectrum are essentially Gaussian in shape. This is mainly due to statistical processes and electronic noise in the detector, which contribute to the detector's energy resolution. It is also partly due to energy degradation from scattering, together with absorption on the low-energy side of the peak, and the effect of 'accidental summing' on the high-energy side of the peak. The latter effect is due to the accidental time-coincidence between events in the detector. Backscattering from metals and other absorbers close to the detector also contribute to the observed spectrum.

Source–detector geometry

Both source thickness and source type (i.e. point, line, or broad) affect the shape of the observed spectrum. Gregory & Horwood (1961) showed that with increasing source thickness there is a greater build-up of the Compton continuum. The photopeaks—which are the distinguishing characteristic of all spectra—are reduced relative to the Compton background. This effect is most severe in the low-energy region of the spectrum, since low-energy photons are more easily attenuated than high-energy photons. Also, the build-up due to Compton scattering is greatest in the low-energy region of the spectrum. A similar change in spectrum shape is seen between spectra from point and broad sources; i.e. with broad sources, greater Compton scattering in the sources themselves results in a build-up of the Compton continuum.

Radiation from the ground is attenuated by material between the source and the detector, as well as within the source itself (e.g. barren regolith, vegetation, moisture, and air). Again, with increasing attenuation the photopeaks diminish relative to the energy continuum because of scattered radiation. However, the attenuation of low-energy radiation is greater than that of high-energy radiation, with the result that even with increased energy degradation due to scattering, the total flux at all energy levels is reduced for increasing source–detector distances or increasing cover. Mass-attenuation coefficients and half-thicknesses for various gamma-ray energy levels in air, water, and concrete are given in Table 4 (Grasty 1979). The effect of detector height on total flux is also important. For example, a 10 per cent change in height at 100 m will cause an 8 per cent change in the measured total-count count rate.

Measured spectra are thus complex functions of many variables. In addition to the concentration and geometry of the source, the spectra are also functions of the height of the detector above the ground, the thickness of any non-radioactive overburden, and the response function of the detector. Typical examples of K U, and Th spectra that would be recorded at airborne height with a long integration time are shown in Figures 8, 9, & 10. These were recorded on the ground using specially constructed radioactive sources. Wood was used to shield the detectors from the sources, thus simulating the attenuation of the gamma rays by air. The measured spectra are continuous functions of energy. A comparison with the simulated fluxes (Figs 5, 6, 7—note log scale on ordinates) illustrates the large effect the detector response has on the measured data. Obviously, the detector response must be considered in the calibration of airborne spectrometers and processing of data.

Environmental effects

Environmental factors that can influence gamma-ray spectrometry include non-radioactive overburden, air temperature and pressure, precipitation, temperature-inversion layers and air movements in the lower atmosphere, and soil moisture.

Barren overburden, because of its high density, can dramatically reduce the radiation output from the Earth's surface. Just 2 cm of cover can reduce it by 35 per cent. In some areas, dense vegetation may have the same capacity to shield the source of radiation as 50 m of air. The trunks of trees in dense forest will have a collimating effect on radiation from the ground. Changing temperature and pressure can lead to a change in air density by up to 30 per cent. This translates into a corresponding change in height correction factors. The effect of Rn trapped in temperature-inversion layers close to the ground under early morning still-air conditions was mentioned earlier. This can adversely affect estimates of background and, ideally, flying should only commence once thermal activity has thoroughly mixed the radon through the lower atmosphere.

Table 4. Mass attenuation coefficient and half-thickness for various gamma-ray energies in air, water, and concrete (after Grasty 1979).

	Mass-attenuation coefficient (cm^2/g)			*Half-thickness*[a]		
Photon energy (MeV)	*Air*[b]	*Water*	*Concrete*[c]	*Air*[d] *(m)*	*Water (cm)*	*Concrete (cm)*
0.01	4.82	4.99	26.5	1.11	0.139	0.01
0.10	0.151	0.168	0.171	35.5	4.13	1.62
0.15	0.134	0.149	0.140	40.0	4.65	1.98
0.20	0.123	0.136	0.125	43.6	5.10	2.22
0.30	0.106	0.118	0.107	50.6	5.87	2.59
0.40	0.0954	0.106	0.0957	56.2	6.54	2.90
0.50	0.0868	0.0966	0.0873	61.8	7.18	3.18
0.60	0.0804	0.0894	0.0807	66.7	7.75	3.43
0.80	0.0706	0.0785	0.0708	75.9	8.83	3.92
1.0	0.0635	0.0706	0.0637	84.4	9.82	4.35
1.46	0.0526	0.0585	0.0528	102	11.8	5.25
1.5	0.0517	0.0572	0.0519	104	12.1	5.34
1.76	0.0479	0.0532	0.0482	112	13.0	5.75
2.0	0.0444	0.0493	0.0447	121	14.1	6.20
2.62	0.0391	0.0433	0.0396	137	16.0	7.00
3.0	0.0358	0.0396	0.0365	150	17.5	7.60

[a] Thickness of material that reduces the intensity of the beam to half its initial value.

[b] 75.5% N, 23.2% O, 1.3% Ar by weight.

[c] For compositions of typical concrete see Hubbel & Berger (1968). Density of concrete is 2.5 g/cm^3.

[d] For air at 0°C and 76 cm of Hg with a density of 0.001293 g/cm^3.

The effect of rainfall is complicated. In general, a 10 per cent increase in soil moisture will decrease the radiation flux from the surface by about the same amount. But for U estimation, the effect of rainfall is one of competing effects. The daughter products of airborne Rn attach themselves to dust particles in the atmosphere. The radioactive precipitation of these particles by rain can lead to apparent increases of more than 2000 per cent in U ground concentration (Charbonneau & Darnley 1970). Surveying should thus cease in areas of recent rainfall until anomalous surface activity has had a chance to decay (about 3 hours). However, Rn escapes more freely from dry soil than from wet soil. High moisture content can actually lead to an increase in the radiation output due to U, because of a build-up of Rn in the soil.

Basic models

The mathematical modelling of gamma-ray fields provides an insight into the physics of the airborne gamma-ray spectrometric method. This insight is important because it provides the necessary tools for effective survey design and an understanding of the physics required for data processing and interpretation.

Physical models

Perhaps the simplest approach to the modelling of gamma-ray fields is a semi-empirical one based on monoenergetic (i.e. unscattered) radiation. A radiation intensity law for an ele-

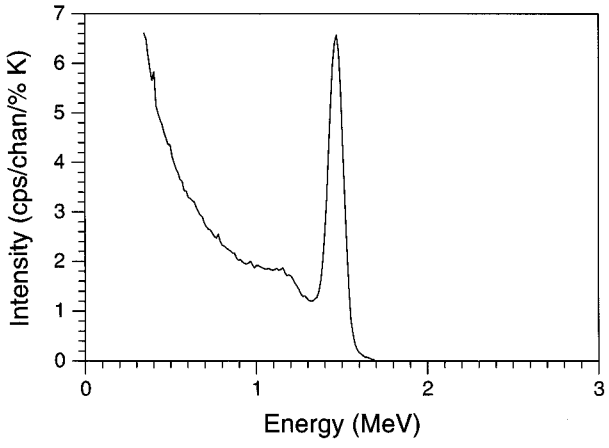

Figure 8. Simulated potassium spectrum at 100 m altitude with a large integration time.

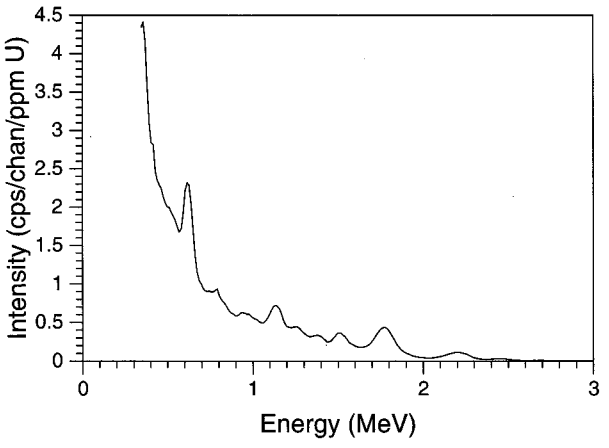

Figure 9. Simulated uranium spectrum at 100 m altitude with a large integration time.

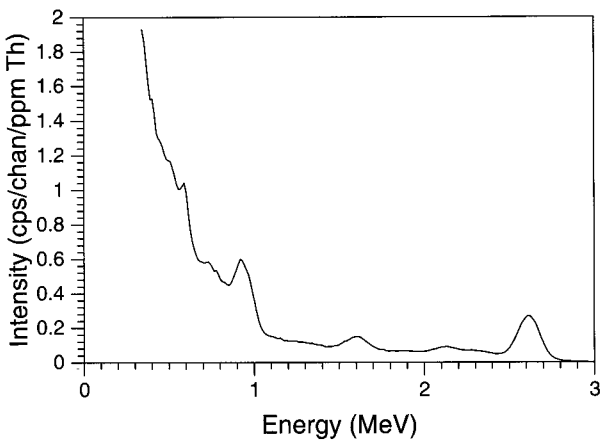

Figure 10. Simulated thorium spectrum at 100 m altitude with a large integration time.

mentary point source is either assumed or determined by laboratory experiment. This expression is then integrated over various geometries to obtain the intensities due to the required sources. For a collimated beam of radiation intensity, I, the amount of radiation, dI, absorbed by an absorber of thickness dx is proportional to both I and dx (Grasty 1979). Thus

$$dI = -\mu I dx \tag{4}$$

where μ is called the linear attenuation coefficient and is characteristic of the absorbing medium and the energy of the radiation. If $I=I_0$ for no absorber present (x=0), then

$$I = I_0 e^{-\mu x} \tag{5}$$

which is the classical law of absorption. This relationship has been verified experimentally (Fano 1953).

However, gamma rays are also subject to the inverse-square law of attenuation for point sources of electromagnetic radiation. Thus, for monoenergetic radiation from an isotropic point source at a distance r, from the detector, we have

$$I \propto \frac{e^{-\mu r}}{r^2} \tag{6}$$

Consider now a two-layer model with the Earth as an infinite half-space with a constant density and radioelement concentration overlain by non-radioactive air of constant density (Figure 11). Assume, also, that the detector at point P presents an equal cross-sectional area in all directions and has an efficiency which is not directionally dependent. Then, the monoenergetic radiation intensity, dI, due to a photopeak of intensity E_0 from gamma-ray emissions by a volume element dV within the Earth is given by (Clark et al. 1972)

$$dI = \frac{A\varepsilon}{4\pi R^2} e^{-\mu_e r_e} e^{-\mu_a r_a} N dV \tag{7}$$

where A = effective cross-sectional area of the detector

ε = photopeak efficiency of the detector for gamma rays of energy E_0

μ_e, μ_a = linear attenuation coefficients for the Earth and air respectively

r_e, r_a = the distances through the Earth and air that the gamma rays travel ($R=r_a+r_e$)

Equation 7 can then be integrated over various geometries to obtain the photopeak response due to a range of source types. For example, the radiation due to a thick circular source expressed as a percentage of the radiation due to an infinite source is given by (Grasty 1987)

$$P = 100\left(\frac{E_2(\mu h) - \cos\varphi E_2\left(\frac{\mu h}{\cos\varphi}\right)}{E_2(\mu h)}\right) \tag{8}$$

where h is the detector height above ground level, μ is the linear attenuation coefficient of gamma rays in air, E_2 is the exponential integral of the second kind, and the circular source subtends an angle of 2φ at the detector.

This type of formulation has been used in several 'fields of view' type investigations, where an insight into the response of the detector system to sources of various geometry is sought (e.g. Duval et al. 1971; Grasty et al. 1979; Tewari & Raghuwanshi 1987). Figure 12 shows the percentage of the infinite source yield for Th gamma rays (^{208}Tl) at 2.61 MeV as a function of source radius. A linear attenuation coefficient for air of 0.00505 m^{-1} and detector height of 100 m have been used. This shows that at 100 m height, less than 40 per cent of the infinite source yield originates from a source with a radius of 100 m, and over 20 per cent of the measured photons for an infinite source originate at lateral distances greater than 300 m. The 'field of view' represented by a typical airborne sample is thus much larger than the 60 m interval over which samples are typically acquired.

As a second example, the radiation due to a broad source of thickness D expressed as a percentage of the radiation due to a broad source of infinite thickness is given by (Grasty 1987)

$$P = 100\,(1 - E_2(\mu D)) \tag{9}$$

where μ is the linear attenuation coefficient of the source material, and the detector is at ground level. This relationship is illustrated in Figure 13 for Th gamma rays (^{208}Tl) at 2.61 MeV. A source density of 2.2 gm/cm^3 and a mass attenuation coefficient of 0.0396 cm^2/gm (ie. μ=0.0871 cm^{-1}) was used. This shows that over 98 per cent of the radiation comes from the top 35 cm of the Earth's crust. Airborne gamma-ray spectrometry can, therefore, only map the concentration of radioelements in a thin layer at the Earth's surface.

More sophisticated derivations of equations 8 and 9 are available. Grasty et al. (1979) included the effect of the angular sensitivities of cylindrical detectors into the analysis. Tewari & Raghuwanshi (1987) repeated this work using the measured angular sensitivity of the more modern rectangular slab detectors. Models that incorporate both scattered and unscattered radiation are also available. In the latter case , a 'build-up' factor is used to accommodate the component due to scattered radiation (e.g. Gregory 1960; Davis & Reinhardt 1962).

The most comprehensive form of modelling in airborne gamma-ray spectrometry is the simulation of gamma-ray transport. Kirkegaard (1972) developed a numerical method to solve Boltzmann's equation for a two-layer model and, hence, simulate the gamma-ray flux distributions at airborne height (Figs 5, 6 & 7). The main limitation to this type of modelling is the detector response. This is a complicated

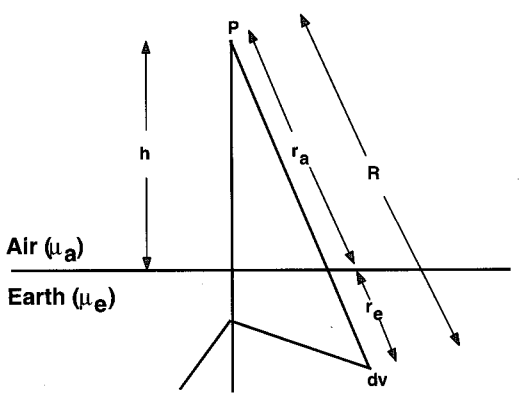

Figure 11. Source detector geometry for the two-layer Earth model. The detector is at point P relative to a source element dV within the Earth.

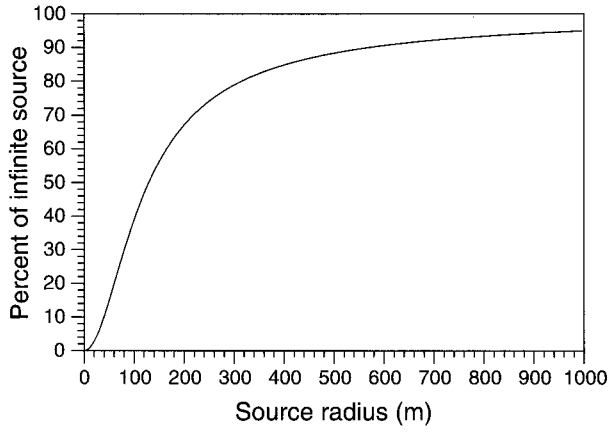

Figure 12. Percentage of the infinite source radiation detected from thick circular sources of varying radius for thorium gamma rays of energy 2.62 MeV and a detector height of 100 m. The angular sensitivity of rectangular slab detectors was included in the analysis.

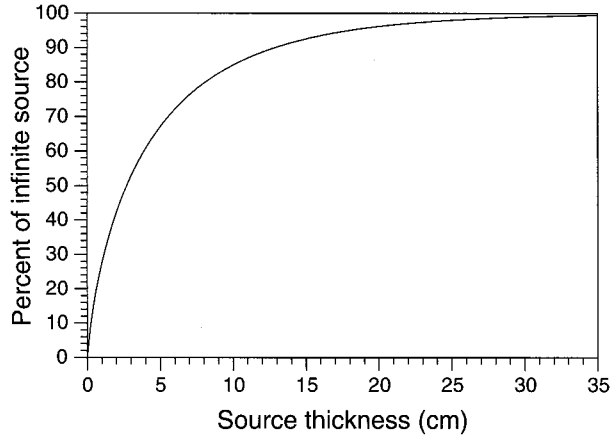

Figure 13. Percentage of the infinite source radiation detected from broad sources of varying thickness for thorium gamma rays of energy 2.62 MeV and a source density of 2.2 gm.cm^{-3}.

function, particularly for airborne spectrometers, where a large proportion of the measured count rates result from scattered radiation, and the effects of partial outscatter, escape peaks, and so on have to be considered. A very large number of Monte Carlo type calculations are required to simulate a response function of adequate detail. Grasty (1979) has suggested that detector response can only be satisfactorily determined through a combination of experiment and Monte Carlo simulations.

Statistical models

Each atomic disintegration during radioactive decay occurs completely independently of every other decay event. This means that the frequency of the radioactive decay, or the frequency of the measured gamma rays associated with the decay, follow a Poisson statistical distribution, ie.

$$P(x) = \frac{\psi^x e^{-\psi}}{x!} \qquad (x = 0,1,2,3,...) \qquad (10)$$

where ψ is a given constant.

A special property of the Poisson distribution often used in gamma-ray spectrometry is that the standard deviation is equal to the square root of the mean count rate:

$$\sigma = \sqrt{n} \qquad (11)$$

where n is the mean count rate. Also, the variance of a distribution is the mean square deviation, equivalent to the square of the standard deviation:

$$v = \sigma^2 = n \qquad (12)$$

The fractional deviation is given by

$$\frac{\sqrt{n}}{n} = \frac{1}{\sqrt{n}} \qquad (13)$$

These relationships give us a convenient means for estimating errors in gamma-ray spectrometry. In other areas of science, errors are usually estimated by repeating the experiment or observation a number of times. In gamma-ray spectrometry, we usually assume that all errors are due to the random nature of radioactive decay, and the variance is taken to be approximately equal to the number of counts observed. For large count rates, the Poisson distribution becomes more normal and, for mean count rates greater than 20, the Poisson and normal distributions are almost identical (Dickson 1980). Under these circumstances it is appropriate to use the weighted least-squares method for the inversion of over-determined systems in gamma-ray spectrometry.

Airborne surveying

Typically, a regional airborne geophysical survey would be flown with 400 m line spacing and at a flying height of between 80 and 100 m. Both gamma-ray spectrometric and magnetic data are usually recorded on these surveys. The line spacing is a compromise between the desired resolution of the data, and the cost of the survey. The flying height is usually related to the line spacing, but is limited by safety considerations. The speed of the aircraft is usually about 50–60 m/s for fixed-wing surveys, but can be appreciably slower for helicopter surveys. There is obviously a trade-off in data acquisition between the measured count rates and, hence, the accuracy of the measurements, sampling time, aircraft speed, and spatial resolution of the data. 'Fields of view' type calculations, using equations such as number 8 above, can be used to estimate the effective coverage for various flying heights. The field of view of the spectrometer is wider at greater heights, but the quality of the gamma-ray spectrometric data improves dramatically as the elevation of the detector decreases, since the fall-off in intensity of radiation with height is roughly exponential. But the survey parameters are almost always optimised for the acquisition of magnetic data, which have traditionally been viewed as the primary exploration and mapping tool.

Modern airborne gamma-ray spectrometric data acquisition systems for regional mapping would comprise a multichannel spectrometer capable of measuring at least 256 channels of data in the energy range 0–3 MeV, and a detector volume of not less than 33 litres of NaI (Tl) crystal. Even with this volume of crystal, multichannel count rates are low. A typical spectrum from one of these regional surveys is shown in Figure 14. The conventional approach to the acquisition and processing of airborne gamma-ray spectrometric data is to monitor four relatively broad spectral windows (Table 5). Windows centred on the 1.46 MeV (K), 1.76 MeV (U) and 2.62 MeV (Th) photopeaks (Fig. 15) have been generally accepted as the most suitable for the measurement of K, U and Th. The total-count window gives a measure of total radioactivity.

The K, U and Th windows are centred on the highest energy diagnostic photopeak for each of the three radioelements. This is significant, since only high-energy photons are able to penetrate in significant numbers to airborne heights, and they are also less susceptible to variations in source geometry or the height of the detector than lower energy photons.

Multichannel data were once used only for monitoring equipment performance, but are now, increasingly, being used for energy calibration of data during processing and for

Table 5. Standard windows for natural radioelement mapping (IAEA 1991). The energy of the photopeak being monitored is shown in brackets after each nuclide.

Window	*Nuclide*	*Energy range (MeV)*
Total Count	–	0.4–2.81
Potassium	^{40}K (1.460 MeV)	1.370–1.570
Uranium	^{214}Bi (1.765 MeV)	1.660–1.860
Thorium	^{208}Tl (2.614 MeV)	2.410–2.810

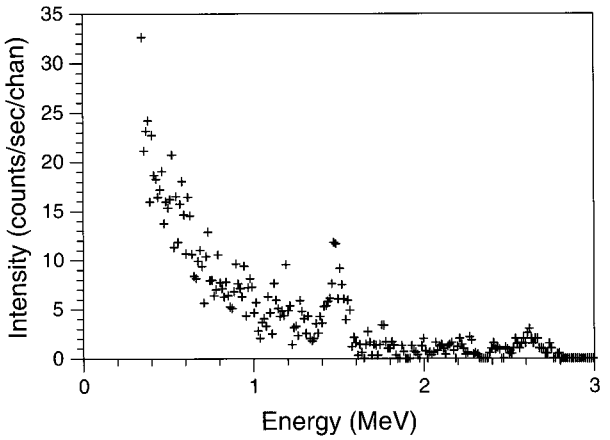

Figure 14. A typical gamma-ray spectrum recorded at 100 m altitude with a 1 s integration time. There are 256 channels between 0 and 3 MeV, giving a channel width of about 11.7 keV.

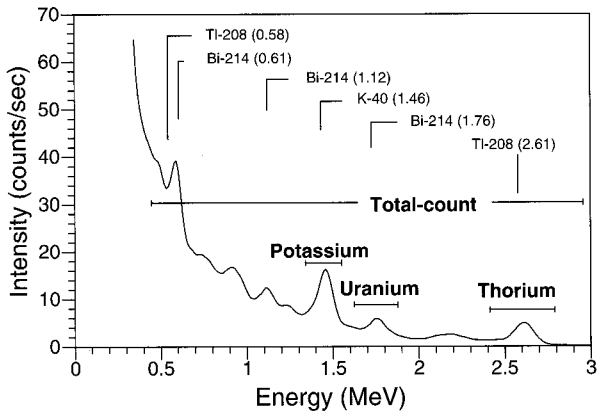

Figure 15. A typical gamma-ray spectrum recorded at 100 m altitude with a large integration time, showing prominent photopeaks and the positions of the conventional 3-channel windows.

estimation of gamma-ray background. The observed spectrum can be considered as the sum of three terrestrial and three background components as follows:

$$I_{obs} = I_K + I_U + I_{Th} + I_{air} + I_{cos} + I_{rad} \quad (14)$$

where I_K, I_U and I_{Th} are the spectra of K and the U and Th decay series, and I_{air}, I_{cos} and I_{rad} are, respectively, the aircraft, cosmic and atmospheric radon background components.

Calibration and data processing for airborne gamma-ray spectrometry are described by Minty et al. (1997). Briefly, the data are processed as follows. The measured spectra are corrected for equipment dead time and then energy calibrated to correct for energy drift in the spectrometer. The background components are then estimated and removed. At this point, the spectra are summed over the conventional windows for further processing. Each elemental window count rate (Fig. 15) is corrected for counts due to the other radioelements (channel interaction correction or 'stripping'). These background-corrected and stripped count rates are then corrected for variations in the height of the detector (height correction) and reduced to elemental concentrations on the ground. For many of the corrections, the approach taken to calibration is empirical. We view the source and detector as a single system and measure its response, for example, to changes in aircraft height (to obtain height attenuation coefficients) and sources of known geometry and concentration (to obtain sensitivity coefficients). It is important to realise, however, that these empirically determined constants are only valid for the source and source–detector geometry used in the calibration process.

Conclusion

The purpose of this paper has been to review the fundamentals of airborne gamma-ray spectrometry. A knowledge of these is essential for an understanding of the calibration of airborne gamma-ray spectrometers and the processing and interpretation of airborne gamma-ray spectrometric data, which are covered elsewhere in this volume (Minty, et al. 1997; Dickson & Scott 1997).

The paper has reviewed basic radioactivity and the source of gamma-radiation, and discussed the interaction of gamma rays with matter, the response of an airborne detector system, and the properties of airborne gamma-ray spectra. The discussions have illustrated that the measured spectrum is a complex function of many variables. The approach taken to calibration, therefore, is empirical, i.e. the response of the source–detector system to sources of known concentration and geometry is measured.

References

Aviv, R. & Vulcan, U., 1983. Airborne gamma-ray survey over Israel: the methodology of the calibration of the airborne system. Israel Atomic Energy Commission, Report No. Z.D. 58/82.

Bailey, R.C., 1986. The altitude dependence of terrestrial gamma-ray spectra: A simple model. Geophysics, 51(11), 2108–2116.

Charbonneau, B.W. & Darnley, A.G., 1970. Radioactive precipitation and its significance to high sensitivity gamma-ray spectrometer surveys. Geological Survey of Canada, Paper 70–1, part B, 32–36.

Clark, R.B., Duval, J.S. Jr. & Adams, J.A.S., 1972. Computer simulation of an airborne gamma-ray spectrometer. Journal of Geophysical Research, 77(17), 3021–3031.

Darnley, A.G. & Grasty, R.L., 1971. Mapping from the air by gamma-ray spectrometry. In: Geochemical exploration. Canadian Institute of Mining & Metallurgy, Special Volume 11, 485–500.

Davis, F.J. & Reinhardt, P.W., 1962. Radiation measurements over simulated plane sources. Health Physics, 8, 233–243.

Dickson, B.L. & Scott, K.M., 1997. Interpretation of aerial gamma-ray surveys. AGSO Journal of Australian Geology & Geophysics, 17(2)—this issue.

Dickson, B.H., 1980. Analytic methods for multichannel airborne radiometrics. MSc. thesis, University of Toronto.

Duval, J.S., Cook, B. & Adams J.A.S., 1971. Circle of investigation of an airborne gamma-ray spectrometer. Journal of Geophysical Research, 76, 8466–8470.

Fano, U., 1953. Gamma-ray attenuation, Part I, Basic processes. Nucleonics, 11(8), 8–12.

Foote, R.S., 1969. Improvements in airborne gamma-radiation data analyses for anomalous radiation by removal of environmental and pedologic radiation changes. In: Nuclear techniques and mineral resources. I.A.E.A., Proceedings Series, 187–196.

Grasty, R.L., 1979. Gamma-ray spectrometric methods in uranium exploration—theory and operational procedures. In: Geophysics and geochemistry in the search for metallic ores. Geological Survey of Canada, Economic Geology Report 31, Paper 10B.

Grasty, R.L., 1987. The design, construction and application of airborne gamma-ray spectrometer calibration pads—Thailand. Geological Survey of Canada, Paper 87-10.

Grasty, R.L. & Carson, J. M., 1982. Discussion on 'Inversion of gamma-ray data for element abundances' (Crossley, D.J. & Reid, A.B.). Geophysics, 47, 1737–1738.

Grasty, R.L., Kosanke, K.L. & Foote, R.S., 1979. Fields of view of airborne gamma-ray detectors. Geophysics, 44(8), 1447–1457.

Gregory, A.F., 1960. Geological interpretation of aeroradiometric data. Geological Survey of Canada, Bulletin 66.

Gregory, A.F. & Horwood, J.L., 1961. A laboratory study of gamma-ray spectra at the surface of rocks. Department of Energy, Mines & Resources, Ottawa, Mines Branch Research Report R85.

Heath, R.L., 1964. Scintillation spectrometry. Gamma-ray spectrum catalogue, 2nd Edition, Volumes 1 and 2: U.S.A.E.C. Research and Development Report IDO–16880–1, Physics T.I.D.–4500 (31st edition).

Hubbell, J.H. & Berger, M.J., 1968. Attenuation coefficients, energy absorption coefficients, and related quantities. Engineering Compendium on Radiological Shielding, v. 1. Springer Verlag, Berlin.

IAEA, 1991. Airborne gamma ray spectrometer surveying. International Atomic Energy Agency, Technical Report Series, No. 323.

Ivanovich, M. Harmon, R.S. (editors), 1982. Uranium series disequilibrium: applications to environmental problems. Clarendon Press, Oxford.

Kirkegaard, P., 1972. Double P1 calculation of gamma-ray transport in semi-infinite media. Danish Atomic Energy Commission, Research Establishment Riso, Report Riso-*M-1460.*

Kirkegaard, P. & Lovborg, L. , 1974. Computer modelling of terrestrial gamma-radiation fields. Riso Report No. 303.

Kogan, R.M., Nazarov, I.M. & Fridman, Sh.D., 1969. Gamma spectrometry of natural environments and formations. Translation 1971 by Israel Program for Scientific Translations Ltd. No. 5778, available from the U.S. Dept. of Commerce, Nat. Tech. Inf. Ser., Springfield, Va., 22151, 337 p.

Minty, B.R.S., Luyendyk, A.P.J. & Brodie, R.C., 1997. Calibration and data processing for airborne gamma-ray spectrometry. AGSO Journal of Australian Geology & Geophysics, 17(2)—this issue..

Tewari, S.G. & Raghuwanshi, S.S., 1987. Some problems on the range of investigation in airborne gamma-ray spectrometry. Uranium, 4(1), 67–82.